Research paper

Protective effect of dioscin against doxorubicin-induced cardiotoxicity via adjusting microRNA-140-5p-mediated myocardial oxidative stress

Lisha Zhao[1], Xufeng Tao[1], Yan Qi[1], Lina Xu, Lianhong Yin, Jinyong Peng[*]

College of Pharmacy, Dalian Medical University, Western 9 Lvshunnan Road, Dalian 116044, China

ARTICLE INFO

ABSTRACT

Clinical application of doxorubicin (DOX) is limited because of its cardiotoxicity. Thus, exploration of effective lead compounds against DOX-induced cardiotoxicity is necessary. The aim of the present study was to investigate the effects and possible mechanisms of dioscin against DOX-induced cardiotoxicity. The *in vitro* model of DOX-treated H9C2 cells and the *in vivo* models of DOX-treated rats and mice were used in this study. The results showed that discoin markedly increased H9C2 cell viability, decreased the levels of CK, LDH, and improved histopathological and electrocardio- gram changes in rats and mice to protect DOX-induced cardiotoxicity. Furthermore, discoin significantly inhibited myocardial oxidative insult through adjusting the levels of in-tracellular ROS, MDA, SOD, GSH and GSH-Px *in vitro* and *in vivo*. Our data also indicated that dioscin activated Nrf2 and Sirt2 signaling pathways, and thereby affected the expression levels of HO-1, NQO1, Gst, GCLM, Keap1 and FOXO3a through decreasing miR-140-5p expression level. In addition, the level of intracellular ROS was significantly increased in H9C2 cells treated by DOX after miR-140-5p mimic transfection, as well as the down-regulated expression levels of Nrf2 and Sirt2, which were markedly reversed by dioscin. In conclusion, our data suggested that dioscin alleviated DOX-induced cardiotoxicity through modulating miR-140-5p-mediated myo-cardial oxidative stress. This natural product should be developed as a new candidate to alleviate cardiotoxicity caused by DOX in the future.

1. Introduction

Doxorubicin (DOX), an efficient chemotherapeutic drug, is widely used in clinical for cancer treatment [1,2]. Unfortunately, this drug can cause acute and chronic cardiotoxicity including tachycardia, ar-rhythmia, hypotension, transient depression of left ventricular function, and even refractory late-onset cardiomyopathy [3–5]. Moreover, DOX-induced cardiotoxicity will be aggravated in patients with the increased dose of DOX [6]. The incidence of heart failure will increase to 48% when the accumulation dose of DOX climbs to $700 \, \text{mg/m}^2$ [7]. Because of the side effects, the application of DOX is limited despite its potent and effective functions.

In recent years, a large number of researches have indicated that DOX-induced myocardial injury involves in multiple biological pro-cesses including oxidative stress, lipid peroxidation, DNA damage,

mitochondrial injury, apoptosis and autophagy [8,9]. Among them, oxidative stress is a key process in DOX-induced myocardial damage. Briefly, DOX produces massive superoxide anion free radicals ($\cdot O2$) and reactive oxygen species (ROS), and then induces mitochondrial dys-function and cell injury [10,11]. Therefore, inhibiting oxidative stress may be an effective prevention and treatment method against DOX-induced cardiotoxicity.

MicroRNA (miRNA) is a single-stranded non-coding RNA, which can be used as potential drug targets to treat human diseases [12–15]. Previous studies showed that miR-140-5p has the biological activities including regulating adipocyte differentiation, inhibiting cancer growth and modulating Alzheimer's disease [16–18]. Furthermore, our pre-vious work has also proved that miR-140-5p plays an important role in DOX- induced cardiotoxicity by inducing myocardial oxidative stress via targeting nuclear erythroid factor 2-related factor 2 (Nrf2) and

Fig. 1. Dioscin protected H9C2 cells against DOX-induced injury (A) Chemical structure of dioscin. (B) Cytotoxicity of dioscin on H9C2 cells. (C) Effects of dioscin on the cell viability of H9C2 cells induced by DOX. (D) Effects of dioscin (50, 100 and 200 ng/mL) for 12 h pretreatment on the cellular morphology of H9C2 cells by bright image ($\times 100$ magnification). Data are presented as the mean $\pm$ SD (n = 5). $^*p < 0.05$, $^{**}p < 0.01$ compared with DOX group.

silent information regulator factor 2-related enzyme 2 (Sirt2) [19]. In brief, Nrf2 is anchored in the cytoplasm where it binds to kelch like ECH-associated protein 1 (Keap1) under normal circumstances [20]. However, Nrf2 translocates into the nucleus and then activates its target genes through an antioxidant-response element (ARE) when Sirt proteins trigger the separation of Nrf2 and Keap1 [21]. Nrf2 can negatively regulate the dissociation and polymerization with Keap1, therefore adjust the expression levels of some anti- oxidative genes and enzymes against oxidative stress [22]. Sirt2 can regulate oxidative stress through increasing forkhead box O3 (FOXO3a) and superoxide dismutase (SOD), and then decrease ROS levels [23]. Thus, miR-140-5p inhibitor may be a potential candidate for the treatment of DOX-induced cardiotoxicity.

Dioscin (shown in Fig. 1A), a natural steroid saponin, is isolated from various herbs [24]. Pharmacological investigations have shown that dioscin has anti-tumor, anti-fungal and anti-hyperlipidemic activities [25–27]. A large number of previous studies have suggested that dioscin has potent effects against liver fibrosis, renal injury and cerebral ischemia/reperfusion injury [28–32]. Importantly, previous study has also indicated that dioscin can prevent mitochondrial apoptosis and

attenuate oxidative stress in cardiac H9c2 cells [33]. However, no studies have reported the effects and molecular mechanisms of dioscin against DOX-induced cardiotoxicity in our best knowledge.

Therefore, the aim of the present work was to investigate the protective effect of dioscin against DOX-induced cardiotoxicity, and test whether this action was through adjusting miRNA-140-5p-mediated myocardial oxidative stress

2. Materials and methods

2.1. Chemicals and materials

DOX was obtained from Sigma (Santa Clara, CA, USA). Dioscin was obtained from Shanghai Tauto Biochemical Technology Co., Ltd. (Shanghai, China), which was dissolved in 0.5% carboxymethylcellulose sodium (CMC-Na) for *in vivo* experiments and in 0.1% dimethylsulfoxide (DMSO) for *in vitro* tests. Tissue Protein Extraction kit, and Nuclear and Cytoplasmic Protein Extraction kit were all purchased from KEYGEN Biotech. Co., Ltd. (Nanjing, China). ROS assay kit, bicinchoninic acid (BCA) protein assay kit and cell lysis buffer kit were

obtained from Beyotime Institute of Biotechn- ology (Jiangsu, China). Creatine kinase (CK), lactate dehydrogenase (LDH), superoxide dismutase (SOD), malondialdehyde (MDA), glutathione peroxidase (GSH-Px) and glutathione (GSH) detection kits were obtained from Nanjing Jiancheng Institute of Biotechnology (Nanjing, China). 3-(4,5-Dimethylthiazol-2-yl)-2,5-diphenyl tetrazolium bromide (MTT) was provided by Roche Diagnostics (Basel, Switzerland). 4′,6′- Diamidino-2-phenylindole (DAPI) was obtained from Sigma (St. Louis, MO, USA). TransZolTM, TransScript® All-in-One First-Strand cDNA Synthesis SuperMix for qPCR (One-Step gDNA Removal) and TransStart® Top Green qPCR SuperMix were provided by Beijing TransGen Biotech Co., Ltd. (Beijing, China). MicroRNAs Quantitation PCR Kit was obtained from Sangon Biological Engineering Technology & Services Co., Ltd. (Shanghai, China).

2.2. Cytotoxicity of dioscin

The H9C2 cells were obtained from the Shanghai Institutes for Biological Sciences (Shanghai, China), and maintained in DMEM supplemented with 10% FBS in a humidified atmosphere of $5\%CO_2$ and $95\%O_2$ at 37 °C. The cells were plated in 96-well plates at a density of 5×10^4 cells/mL for 24 h before treatment with different concentrations of dioscin (0–1000 ng/mL). The cells in control groups were treated with 0.1% DMSO. Moreover, after 24 h incubation, the cell viabilities were detected by MTT assay. Briefly, MTT (5 mg/mL, 10 μL) solution was added to each well for 4 h incubation at 37 °C, and then the medium was removed. Finally, DMSO (150 μL) was added to dissolve the formazan crystals, and the absorbance was measured at 490 nm by using a POLARstar OPTIMA multi-detection microplate reader (BioRad, San Diego, CA, USA).

2.3. DOX-induced cell injury

The H9C2 cells were seeded in 96-well plates at a density of 5×10^4 cells/mL for 24 h and pretreated with different concentrations of dioscin (0–1000 ng/mL for 24 h before challenged with DOX (5 μM)) for 24 h. The cells in control groups were treated with 0.1% DMSO. Moreover, the cells in DOX group were cultured without dioscin and the cells in control group were cultured in DMEM under normal conditions. Finally, the cell viabilities were detected using the MTT method as described above. Moreover, cell morphologies were imaged using a phase contrast microscope (Nikon, Japan).

2.4. Animals and ethical approval

Male-SD rats weighing 200–250 g (8-weeks old) and male-C57BL/6J mice weighing 18–22 g (4-weeks old) were obtained from the Experimental Animal Center at Dalian Medical University (Dalian, China). All experimental procedures were performed in strict accordance with PR China Legislation Regarding the Use and Care of Laboratory Animals, and all experiments involving animals were approved by the Animal Care and Use Committee of Dalian Medical University. The animals were group-housed with 2–3 rats or mouse per cage on a 12 h light/dark cycle in a temperature-controlled (25 ± 2 °C) room with free access to water and food, and were allowed one week to acclimatize before experiment.

2.5. DOX-induced myocardial injury in vivo

Fifty rats and fifty mice were all randomly divided into two groups: control group (n = 10) and DOX-treated group (n = 40). The animals in DOX groups were intraperitoneally injected with DOX (15 mg/kg/day diluted with 0.9% saline [34,35]), whereas the animals in control groups were intraperitoneally injected with equal volumes of 0.9% saline. After eight days, the animals in DOX-treated groups were randomly divided into four groups (n = 10): model groups and different

doses of dioscin-treated groups (the rats were orally administrated with dioscin at the doses of 60, 30 and 15 mg/kg once daily for seven consecutive days; the mice were orally administrated with dioscin at the doses of 80, 40 and 20 mg/kg once daily for seven consecutive days). The animals in control groups were treated with 0.5% CMC-Na for seven consecutive days. Finally, the electrocardiograms (ECG) of rats and mice were detected before the animals were sacrificed. The serum samples were obtained from blood by centrifugation (3000r/min, 4 °C) for 10 min, and the heart tissues were promptly removed for pathological staining and Western blot assay.

2.6. Measurement of electrocardiograms in rats and mice

The animals were anaesthetized and fixed on the table with the supine position according to the previous method [36]. Subcutaneous needle electrodes of the commercial computer-based ECG device (BL-420F Biological Function Experiment System, Chengdu Thai Union Technology Co, Ltd., China) were connected to the animals, and electrocardiograms were recorded.

2.7. Measurement of CK, LDH, MDA, SOD, GSH and GSH-Px levels

The CK and LDH levels in serum were detected using the commercial kits according to the instructions. In addition, the heart tissues were placed in cold saline (1: 10, w/v), and then homogenized with a homogenizer machine. Next, the supernatant were obtained through centrifuging at 3000r/min for detecting the MDA, SOD, GSH and GSH-Px levels in heart tissues.

2.8. Histopathologic assay

Heart tissues were fixed in 10% formalin and embedded in paraffin, and then the sections were stained with hematoxylin-eosin (H&E) solution. Finally, images of the stained sections were obtained using a light microscope (Nikon Eclipse TE2000-U, Japan) with $200 \times$ magnification.

2.9. Measurement of intracellular ROS

The H9C2 cells were plated in 6-well culture plates at a density of 5×10^4 cells/ mL and treated with dioscin at the concentrations of 50, 100 and 200 ng/mL for 24 h before challenge with 24 h-incubation of DOX. Next, DCFH-DA (10.0 μM, 1.5 mL) was added in the well for 25 min-induction at 37 °C after removing the medium. The samples were ultimately observed by using a fluorescence microscopy (Olympus, Tokyo, Japan) at $200 \times$ magnification.

2.10. Quantification of miR-140-5p

The total microRNA samples in cells and animals were all isolated using the SanPrep Column Micro-RNA Mini-Prep Kit. Reverse transcription was performed using a MicroRNA First Strand cDNA Synthesis Kit, and the levels of mature miRNA were quantified using real-time PCR with a MicroRNAs Quantitation PCR Kit and an ABI 7500 real-time PCR system (Applied Biosystems, USA). The U6 small nucleolar RNA was used for normalization, and the primers for miR-140-5p is CAGT GGTTTTACC- CTATGGTAG.

2.11. Immunofluorescence assay

Immunofluorescence staining for Sirt2 in cells and heart tissues was performed using anti-Sirt2 antibody in a humidified box at 4 °C overnight, and followed by incubation with an Alexa fluorescein-labeled secondary antibody for 1 h at 37 °C. The cell nuclei were stained with DAPI (5.0 μg/mL). Finally, the immunostained samples were imaged by fluorescence microscopy (Olympus, Japan) at $200 \times$ magnification.

Table 1
The information of the antibodies used in the present work.

Antibody	Source	Dilutions	Company
Nrf2	rabbit	1: 800	ABclonal, USA
Keap1	rabbit	1: 1000	Proteintech Group, Chicago, USA
HO-1	rabbit	1: 1000	Proteintech Group, Chicago, USA
NQO1	rabbit	1: 1000	Proteintech Group, Chicago, USA
Gst	rabbit	1: 800	ABclonal, USA
GCLM	rabbit	1: 1000	Abcam, Cambridge, UK
Sirt2	rabbit	1: 1000	Abcam, Cambridge, UK
FOXO3a	rabbit	1: 800	Abcam, Cambridge, UK
GAPDH	rabbit	1: 1000	Proteintech Group, Chicago, USA

2.12. Western blotting assay

The total protein samples from the cells and heart tissues were homogenized using RIPA lysis buffer containing protease and phosphatase inhibitors. The protein concentrations of the samples were determined using a BCA Protein Assay Kit. After determination of the contents, the proteins were separated by SDS-PAGE (8–12%), and then transferred to PVDF membranes (Millipore, Massachusetts, USA). After being blocked with 5% skim milk for 3 h at room temperature, the membranes were incubated with primary antibodies (Table 1) overnight at 4 °C. After addition of the anti-rabbit or anti-mouse secondary antibody for 2 h at room temperature, the protein bands on the membranes were detected using an enhanced chemilumines-cence system and a Bio-Spectrum Gel Imaging System, respectively (UVP, California, USA). Intensity values of the relative protein levels were normalized to GAPDH.

2.13. MiR-140-5p mimic transfection test in vitro

MiR-140-5p mimic transfection was performed to up-regulate the expression level of miR-140-5p. Briefly, the mimic negative control and
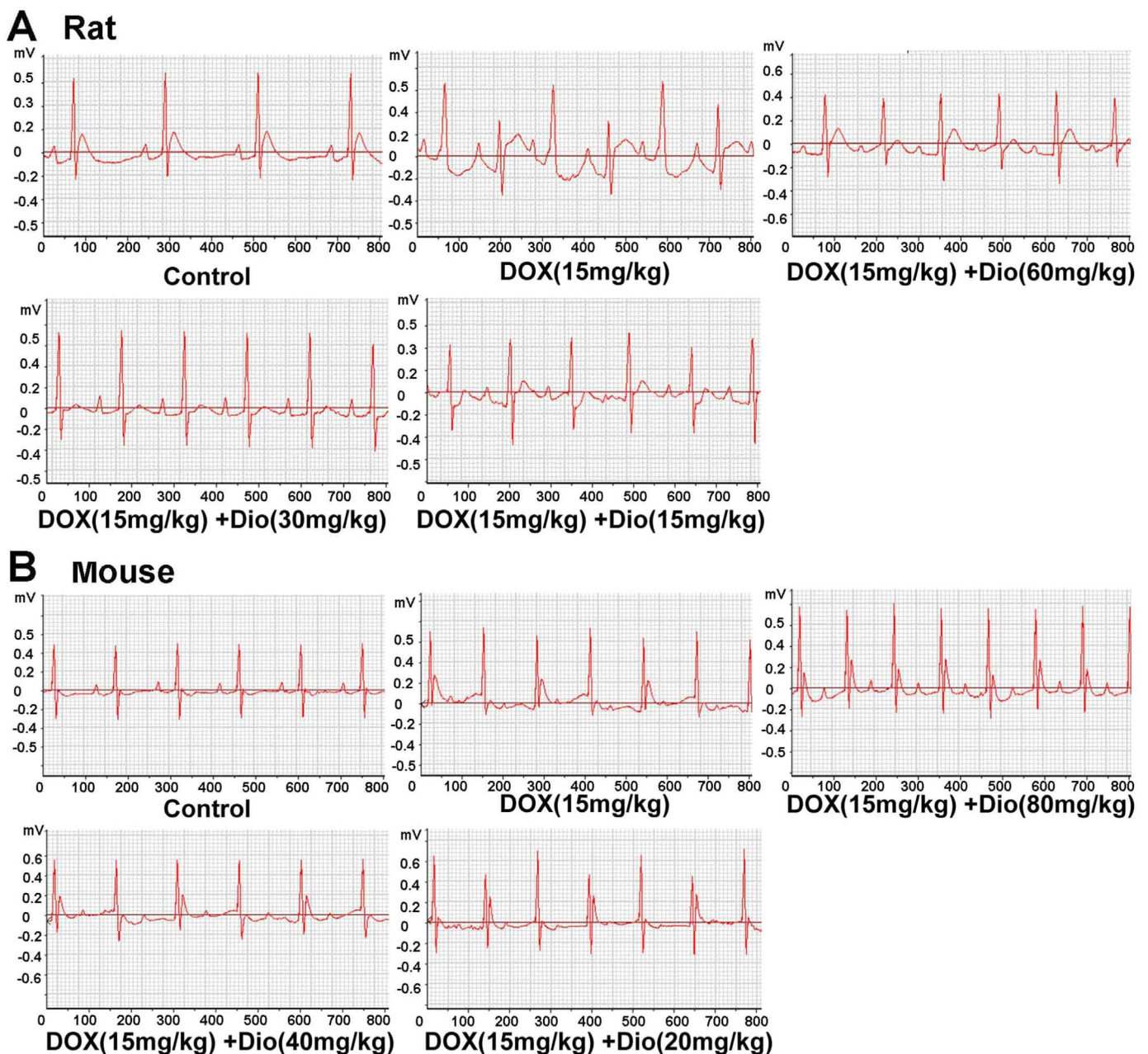
Fig. 2. Dioscin improved DOX-caused electrocardiograms in rats (A) and mice (B).
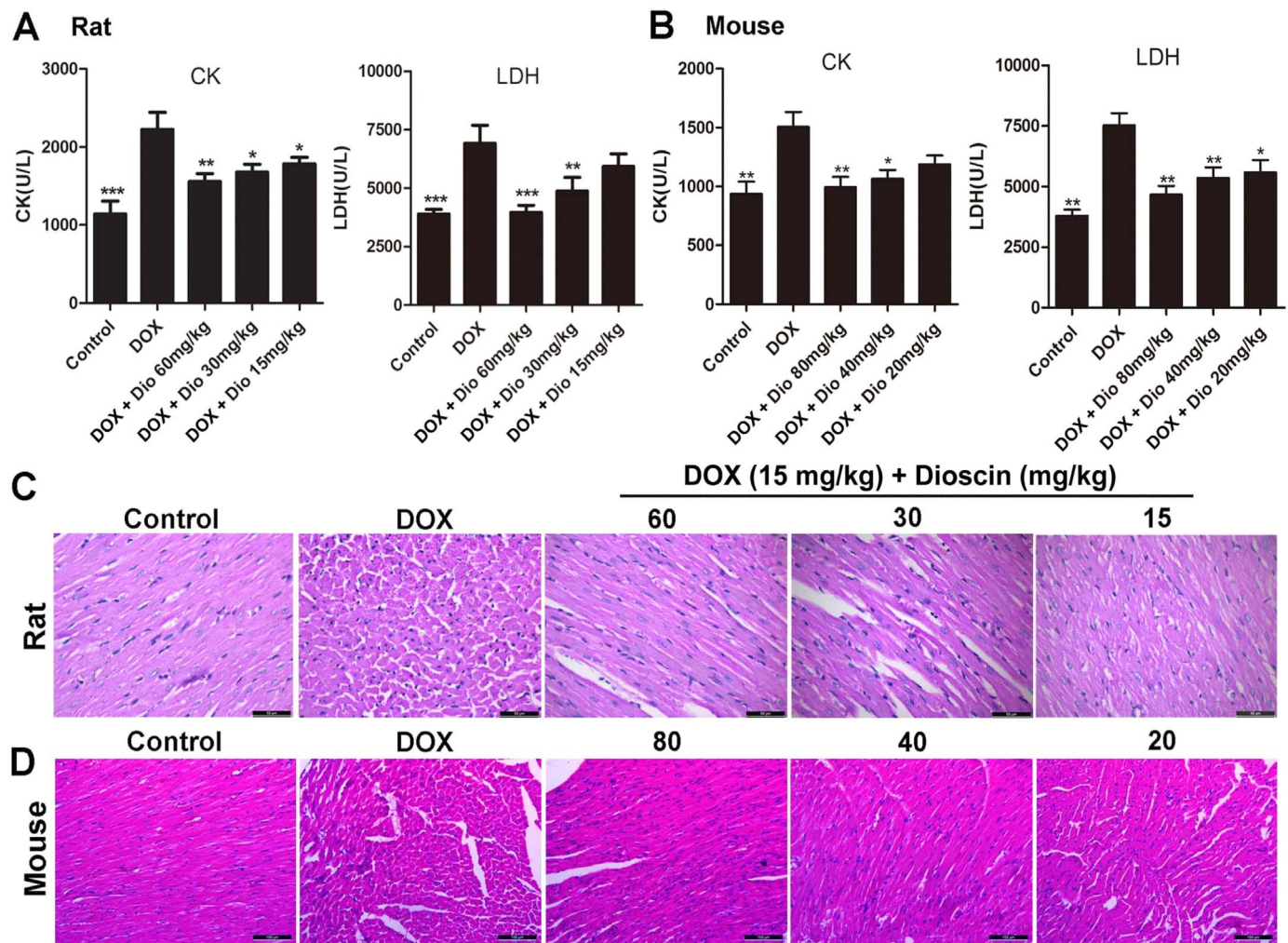
Fig. 3. Dioscin alleviated DOX-induced cardiotoxicity in rats and mice. (A) Effects of dioscin on serum levels of CK and LDH in rats caused by DOX. (B) Effects of dioscin on serum levels of CK and LDH in mice caused by DOX. (C) Effects of dioscin on HE staining images of heart tissues in rats ($\times 200$ magnification). (D) Effects of dioscin on HE staining images of heart tissues in mice ($\times 200$ magnification). Data are presented as the mean $\pm$ SD (n = 10). $^*P < 0.05$, $^{**}p < 0.01$ compared with DOX groups.

miR-140-5p mimic were separately dissolved in Opti-MEM. The solutions were then equilibrated for 5 min at room temperature. Each solution was combined with Lipofectamine 2000 transfection reagent according to the manufacturer's protocol. Then, the solution was mixed gently and allowed to form inhibitor liposomes for 20 min. The H9C2 cells were transfected with the transfection mixture in serum-free cell medium. The cell medium was replaced by fresh medium after incubated at 37 °C for 6 h. Then, the ROS levels, and the expression levels of Nrf2 and Sirt2 were detected after 24 h of administration.

2.14. Data analysis

The data are expressed as the mean $\pm$ standard deviation (SD). Statistical analysis was performed with GraphPad Prism 5.0 software (San Diego, CA, USA). It was performed with one-way analysis of variance (ANOVA) followed by Tukey's post-hoc test when comparing multiple groups; with unpaired t-test when comparing two different groups. Statistical significance was considered to be P < 0.05 or P < 0.01.

3. Results

3.1. Dioscin alleviates myocardial injury in vitro

As shown in Fig. 1B, compared with control group, the viabilities of

H9C2 cells treated with different concentrations of dioscin for 3, 6, 9 and 24 h were not remarkably changed, suggesting that dioscin under the tested concentrations had no significant toxicity to H9C2 cells. Furthermore, the viability of H9C2 cells administrated with 5 μM of DOX was notably decreased as well as the remarkably damaged morphology compared to control group. However, dioscin at the doses of 50, 100 and 200 ng/mL significantly increased the viabilities of H9C2 cells and improved the morphology insult compared with DOX group (Fig. 1C-D). The solvent control of 0.1% DMSO showed no effect to the cells.

3.2. Dioscin alleviates myocardial injury in vivo

As shown in Fig. 2A-B, compared with control groups, the obvious abnormalities in ECG of DOX-treated groups were the changes in ST-segment, which were improved by dioscin. In addition, the serum CK and LDH levels in DOX groups of rats and mice were all obviously increased compared with control groups. However, dioscin significantly decreased the serum CK and LDH levels (Fig. 3A-B). Furthermore, as shown in Fig. 3C-D, HE staining showed that myocardial cells in control groups were neatly arranged with no bleeding, edema and other abnormalities. However, DOX caused myocardial cell injury including obvious myocardial tissue texture unclear, pyknosis and plasma dissolve, which were significantly improved by dioscin. The control solvents including 0.9% saline and 0.5% CMC-Na showed no effects to
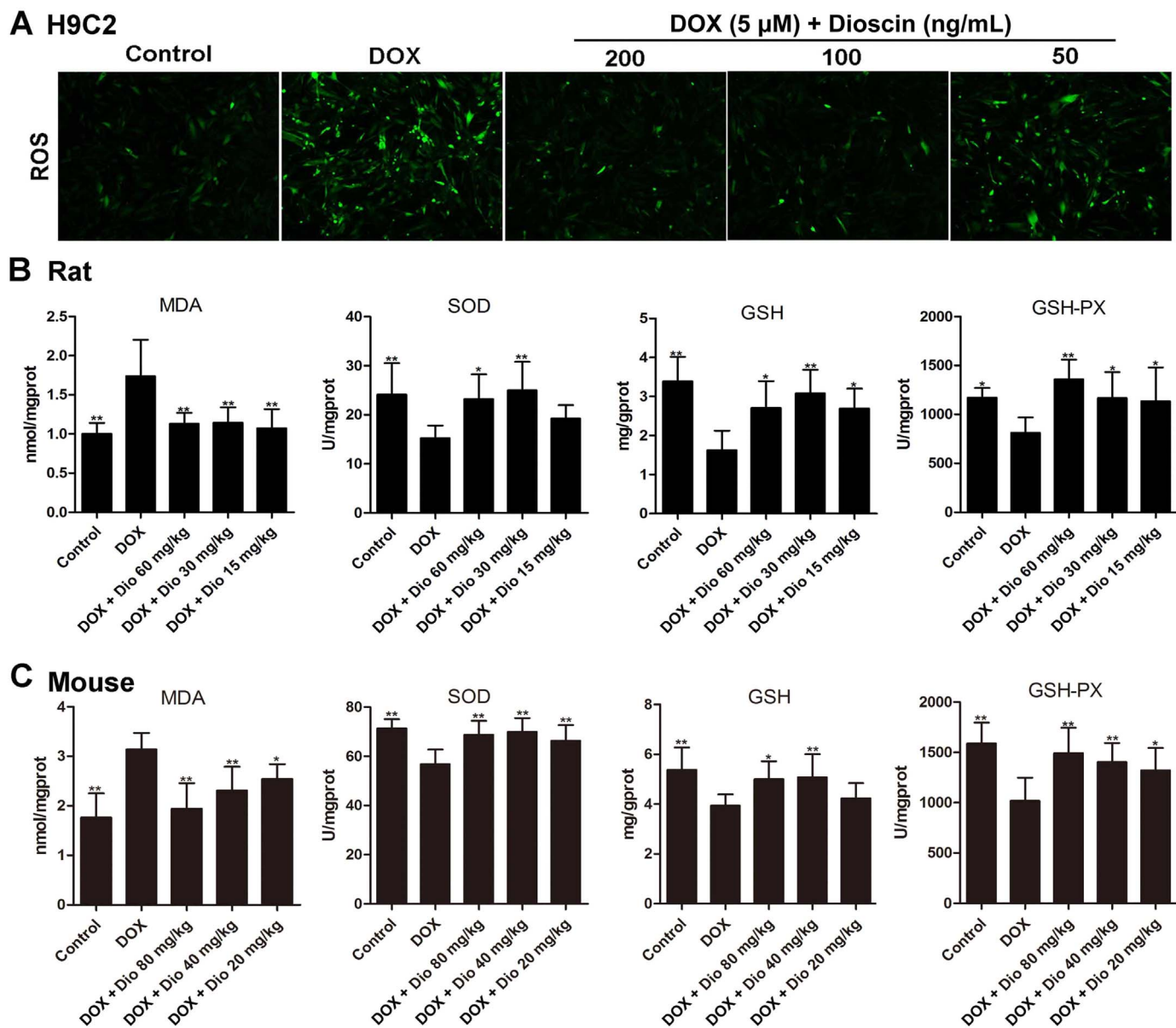
Fig. 4. Dioscin alleviated oxidative stress *in vitro* and *in vivo*. (A) Effects of dioscin on intracellular ROS level in H9C2 cells treated by DOX. (B) Effects of dioscin on the levels of MDA, SOD, GSH and GSH-Px in heart tissues of rats caused by DOX. (C) Effects of dioscin on the levels of MDA, SOD, GSH and GSH-Px in heart tissues of mice caused by DOX. Data are presented as the mean ± SD (n = 10). $^*p < 0.05$, $^{**}p < 0.01$ compared with DOX groups.

animals.

3.3. Dioscin alleviates oxidative damage in vitro and in vivo

As shown in Fig. 4A, compared with control group, the intracellular ROS level in H9C2 cells in DOX group was remarkably increased. However, dioscin markedly decreased ROS level in H9C2 cells compared with model group. In addition, as shown in Fig. 4B-C, compared with DOX groups, MDA levels in heart tissues were significantly decreased, and the levels of SOD, GSH and GSH-Px were markedly increased by dioscin. These results indicated that dioscin significantly alleviated DOX- induced oxidative damage *in vitro* and *in vivo*.

3.4. Dioscin decreases miR-140-5p level and increases Sirt2 level in vitro and in vivo

The results in Fig. 5A revealed that DOX obviously up-regulated the expression levels of miR-140-5p in H9C2 cells and heart tissues of rats

and mice, which were all down-regulated by dioscin. In addition, as shown in Fig. 5B, the expression levels of Sirt2 in H9C2 cells and heart tissues were significantly decreased by DOX based on immunofluorescence assay, which were notably increased by dioscin.

3.5. Dioscin adjusts Nrf2 and Sirt2 signal pathways in vitro and in vivo

As shown in Fig. 6A-C, the expression levels of nuclear Nrf2, cytoplasmic Nrf2, Sirt2 and some downstream proteins in H9C2 cells and heart tissues of rats and mice were assessed by western blotting assay, and the results indicated that the expression levels of nuclear Nrf2, HO-1, NQO1, Gst, GCLM, Sirt2 and FOXO3a were significantly decreased, and the levels of cytoplasmic Nrf2 and Keap1 were markedly increased by DOX compared with control groups *in vitro* and *in vivo*. However, compared with model groups, dioscin significantly increased the expression levels of nuclear Nrf2, HO-1, NQO1, Gst, GCLM, Sirt2 and FOXO3a, and decreased cytoplasmic Nrf2 and Keap1 levels. These results indicated that dioscin increased nuclear translocation of Nrf2 and
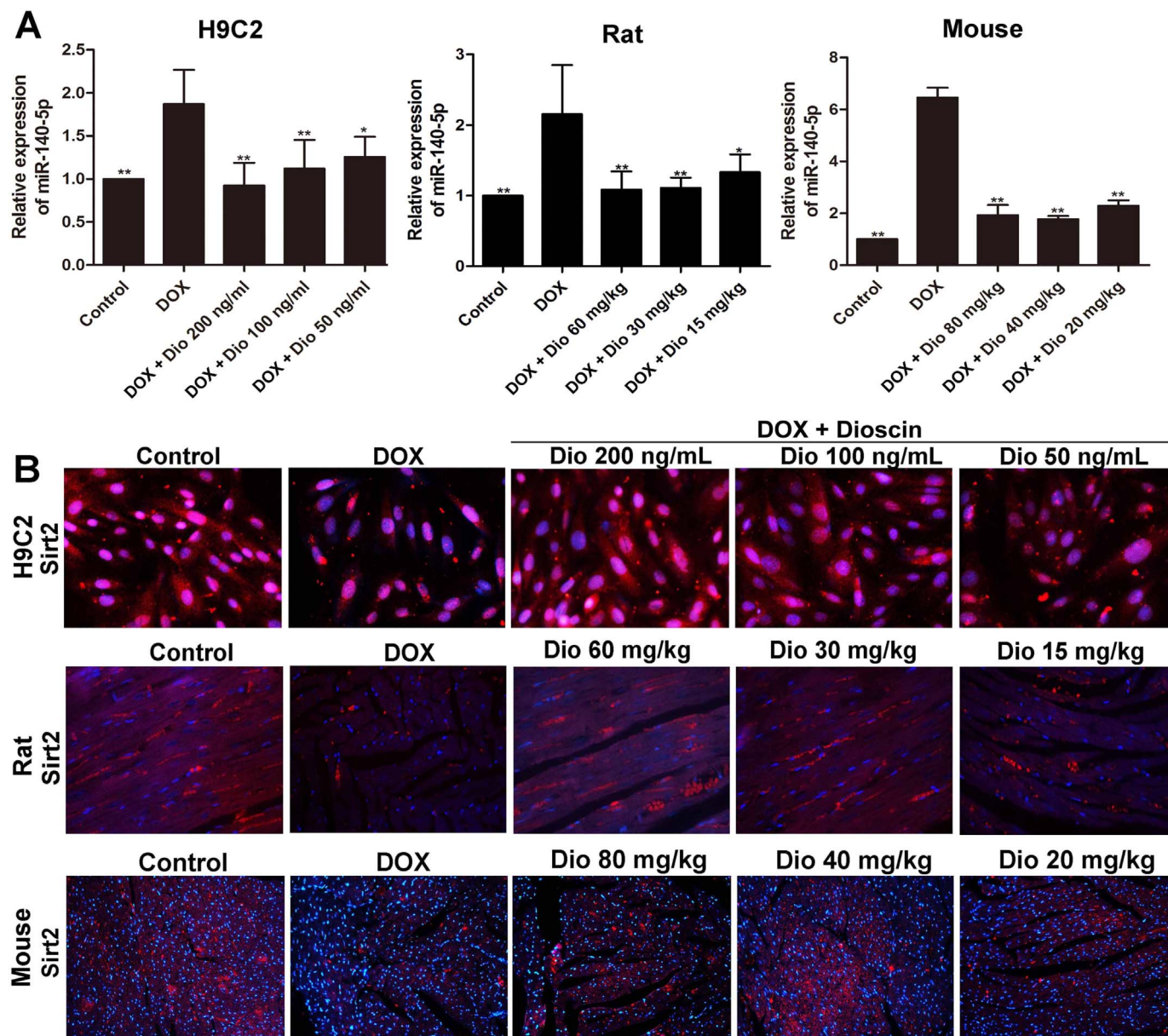
Fig. 5. Dioscin up-regulated Sirt2 level via decreasing miR-140-5p level. (A) Effects of dioscin on miR-140-5p levels *in vitro* and *in vivo* treated by DOX. (B) Effects of dioscin on Sirt2 levels *in vitro* and *in vivo* treated by DOX. Data are presented as the mean ± SD (n = 5). $^*p < 0.05$, $^{**}p < 0.01$ compared with DOX groups.

Sirt2 expression, then affected the expression levels of HO-1, NQO1, Gst, GCLM, Keap1, FOXO3a, and alleviated DOX-caused myocardial oxidative stress.

3.6. Dioscin reverses the effects of miR-140-5p mimics

To further investigate the inhibiting effect of miR-140-5p-mediated signal pathway by dioscin, the method of miR-140-5p mimic was used. As shown in Fig. 7A, transfection with miR-140-5p mimic increased DOX-induced ROS level, which was reversed by dioscin at the dose of 200 ng/mL. Moreover, compared with control group, miR-140-5p mimic transfection notably down-regulated the expression levels of Sirt1 and total Nrf2 in H9C2 cells (Fig. 7B). In addition, as shown in Fig. 7C, compared with miR-140-5p mimic group, the protein levels of Sirt1 and total Nrf2 in H9C2 cells were significantly increased by 200 ng/mL of dioscin.

4. Discussion

DOX belongs to the family of anthracyclines, which has made substantial help since late 1960s in anticancer treatment [37]. However, DOX-induced cardiotoxicity can be observed in animal studies and clinical patients [38,39]. Thus, it is necessary to find active lead compounds against DOX-induced cardiotoxicity. Dioscin, a natural product, shows potent protective effects against multiple organ injuries in our previous studies via regulating oxidative stress through adjusting multiple signal pathways [40–43]. The present study examined the protective effect of dioscin *in vitro* and *in vivo* against DOX-induced cardiotoxicity, and our data indicated that dioscin markedly improved cardiac function, as demonstrated by the improvements of CK, LDH levels, and ECG and histopathological changes of hearts.

A large number of studies have also proved that the underlying mechanisms of DOX-induced cardiotoxicity are closely associated with oxidative stress in myocardial cells [44]. During evolution intrinsic antioxidant system emerges in cells to decrease ROS level and improve
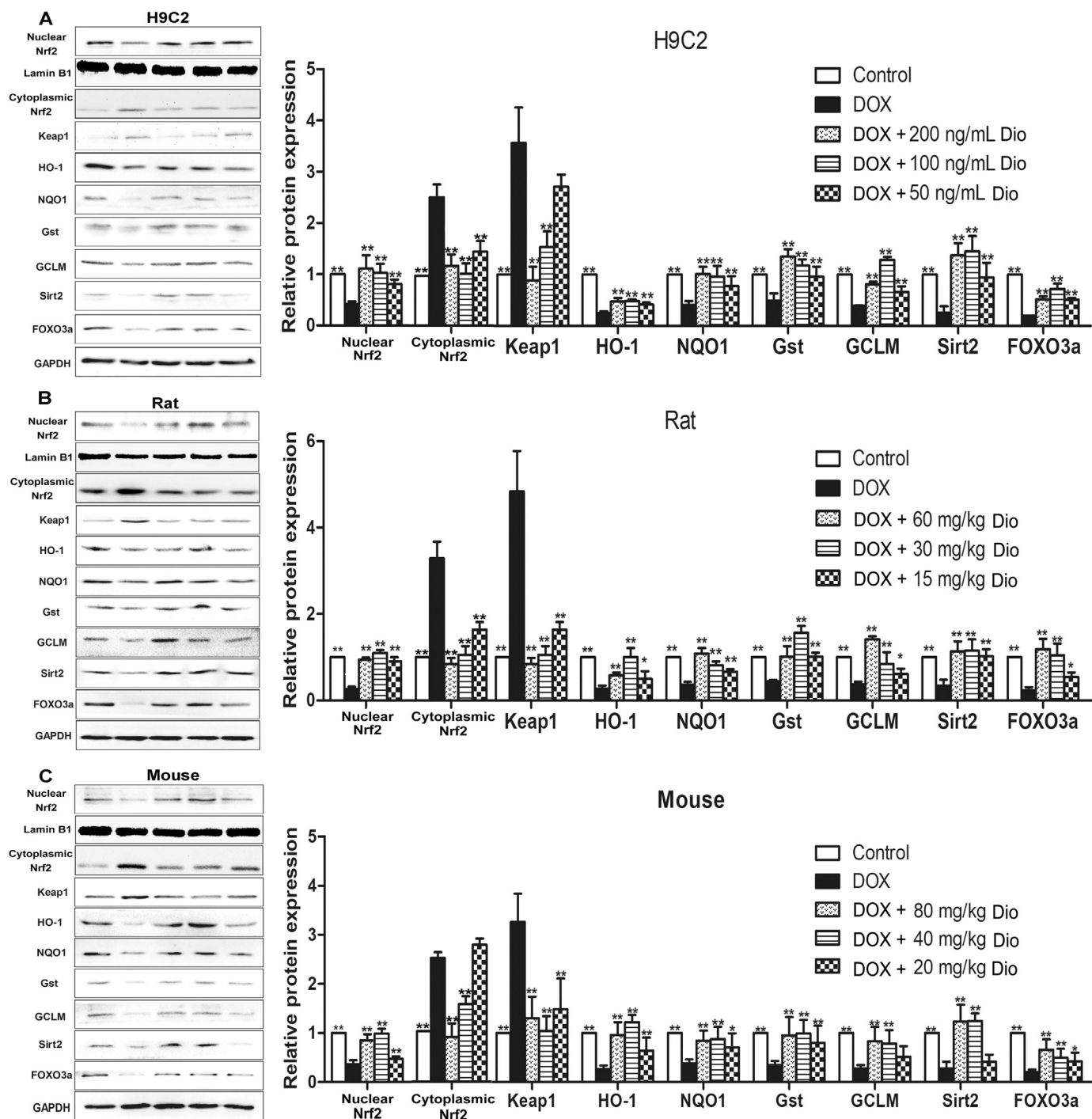
Fig. 6. Dioscin adjusted Nrf2 and Sirt2 signal pathways *in vitro* and *in vivo*. (A) Effects of dioscin on the expression levels of nuclear Nrf2, cytoplasmic Nrf2, keap1, HO-1, NQO1, Gst, GCLM, Sirt2 and FOXO3a in H9C2 cells treated by DOX. (B) Effects of dioscin on the expression levels of nuclear Nrf2, cytoplasmic Nrf2, keap1, HO-1, NQO1, Gst, GCLM, Sirt2 and FOXO3a in rats treated by DOX. (C) Effects of dioscin on the expression levels of nuclear Nrf2, cytoplasmic Nrf2, keap1, HO-1, NQO1, Gst, GCLM, Sirt2 and FOXO3a in mouse treated by DOX. All data are expressed as the mean ± SD (n = 5). $^{*}p < 0.05$, $^{**}p < 0.01$ compared with DOX groups.

cell survival ability. Some important antioxidant enzymes mainly include GSH, GSH-Px and SOD. Among them, GSH and GSH-Px can catalyze the reduction of hydrogen peroxide and other peroxides, and SOD can catalytically reduce O^{2-} to hydrogen peroxide [45,46]. In this paper, the results indicated that dioscin inhibited oxidative damage of myocardium induced by DOX as evidenced by the down-regulated levels of ROS *in vitro* and the up-regulated SOD, GSH, GSH-Px levels *in vivo*. In addition, MDA, an end-product of lipid hydroperoxide and one ROS indicator was significantly decreased by dioscin. Therefore, these results showed that dioscin significantly alleviated DOX-induced

myocardial oxidative damage.

Many signals have been reported to regulate oxidative stress. MiRNA, a kind of small non-coding RNAs (ncRNAs), can regulate gene expression through binding with target mRNA [13–15]. There have growing evidences that miRNAs can be considered as the potential drug targets to treat myocardial insult. MiR-499 can result in the irreversible damage of heart by causing arrhythmia and myocardial hypertrophy [47]. In addition, miR-532-3p and miR-208a have been reported to play important roles in DOX-induced cardiotoxicity [48,49]. Our previous work has also indicated that miR-140-5p targeting Nrf2 and Sirt2-
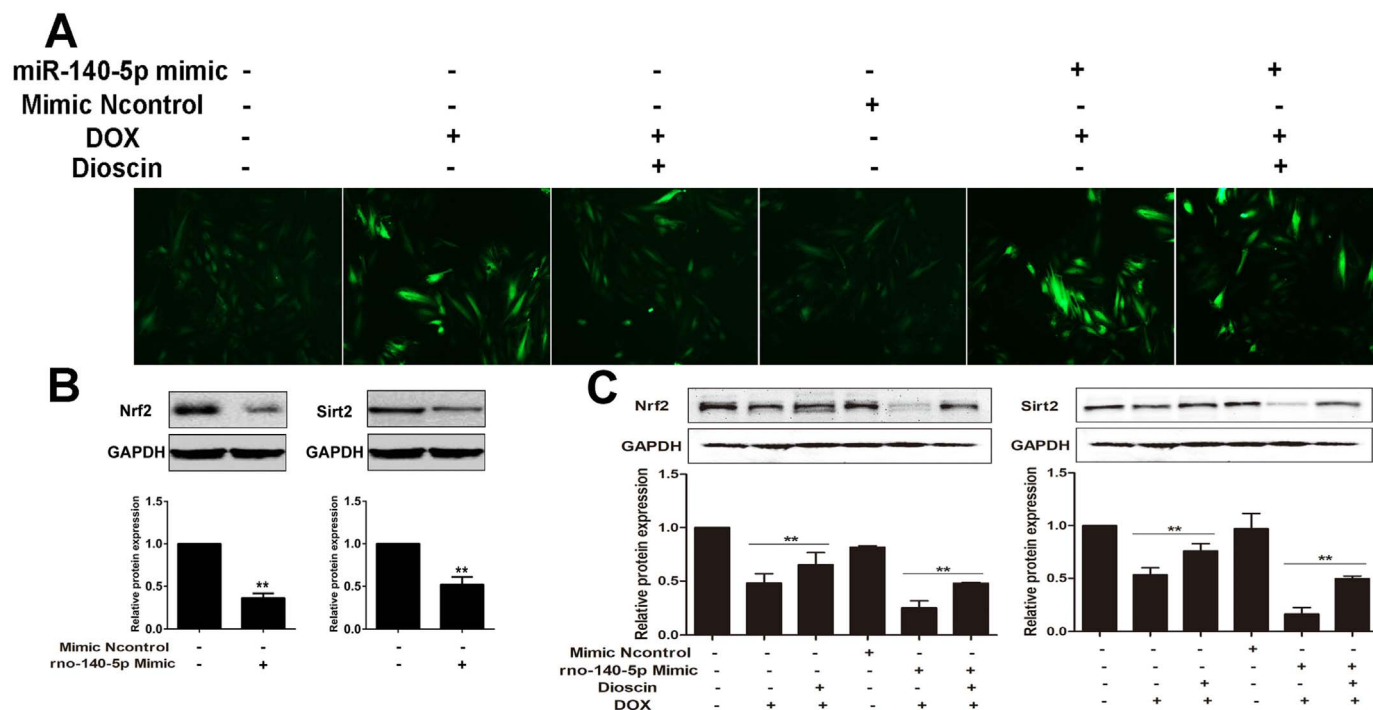
Fig. 7. Dioscin reversed the effect of miR-140-5p overexpression *in vitro*. (A) Effects of dioscin on ROS level in DOX-treated H9C2 cells with transfection of miR- 140-5p mimic. (B) Effects of miR-140-5p mimic on the expression levels of Nrf2 and Sirt2 in H9C2 cells. $^{**}p < 0.01$, compared with control groups. (C) Effects of dioscin on the expression level of Nrf2 and Sirt2 in DOX -treated H9C2 cells with transfection of miR-140-5p mimic. All data are expressed as the mean ± SD (n = 5). $^{**}p < 0.01$, compared with DOX group or DOX + mimic group.

mediated oxidative stress may be the new target for the treatment of DOX-induced cardiotoxicity [16]. Thus, miR-140-5p inhibitor may be a potential candidate to treat DOX-induced cardiotoxicity. In the present work, we found that dioscin markedly inhibited miR-140-5p expression level, and consequently increased the nuclear translocation of Nrf2 and Sirt2 expression, then affected the expression levels of HO-1, NQO1, Gst, GCLM, Keap1, FOXO3a, and alleviated DOX -caused myocardial oxidative stress. Furthermore, the levels of intracellular ROS were significantly increased in H9C2 cells administrated with DOX after miR-140-5p mimic transfection, as well as the changed expression levels of total Nrf2 and Sirt2 signals. However, compared with mimic group, dioscin decreased ROS level, and up-regulated the expression levels of total Nrf2 and Sirt2, suggesting that dioscin reversed the effects of miR-140-5p mimic. Thus, our data demonstrated that dioscin regulated oxidative stress mainly via inhibiting miR-140-5p signaling pathway.

In conclusion, our data showed that dioscin notably decreased DOX-induced cardiotoxicity by adjusting miRNA-140-5p-mediated myocardial oxidative stress, which should be developed as a new potential candidate for clinical therapy. Of course, the deeply mechanisms and clinical applications of this natural product against DOX-induced cardiotoxicity are needed further study.

Acknowledgments

Competing interests

The authors declare no competing financial interests.

References

[1] S. Gergely, C. Hegedűs, P. Lakatos, K. Kovács, R. Gáspár, T. Csont, et al., High throughput screening identifies a novel compound protecting cardiomyocytes from doxorubicin- induced damage, Oxid. Med. Cell Longev. 2015 (2015) 178513.
[2] C.E. DeSantis, R.L. Siegel, A.G. Sauer, K.D. Miller, S.A. Fedewa, K.I. Alcaraz, et al., Cancer statistics for African Americans, 2016: progress and opportunities in reducing racial disparities, CA Cancer J. Clin. 66 (2016) 290–308.
[3] S.E. Lipshultz, N. Rifai, V.M. Dalton, D.E. Levy, L.B. Silverman, S.R. Lipsitz, The effect of dexrazoxane on myocardial injury in doxorubicin-treated children with acute lymphoblastic leukemia, N. Engl. J. Med. 351 (2004) 145–153.
[4] S.Y. Wen, C.Y. Tsai, P.Y. Pai, Y.W. Chen, Y.C. Yang, R. Aneja, et al., Diallyl trisulfide suppresses doxorubicin-induced cardiomyocyte apoptosis by inhibiting MAPK/ NF-κB signaling through attenuation of ROS generation, Environ. Toxicol. 33 (2018) 93–103.
[5] M.W. Bloom, C.E. Hamo, D. Cardinale, B. Ky, A. Nohria, L. Baer, et al., Cancer therapy- related cardiac dysfunction and heart failure, Circ. Heart Fail. 9 (2016) e002661.
[6] S. Christiansen, R. Autschbach, Doxorubicin in experimental and clinical heart failure, Eur. J. Cardiothorac. Surg. 30 (2006) 611–616.
[7] D.L. Li, J.A. Hill, Cardiomyocyte autophagy and cancer chemotherapy, J. Mol. Cell Cardiol. 71 (2014) 54–61.
[8] R.C. Chen, X.D. Xu, X. Zhi Liu, G.B. Sun, Y.D. Zhu, X. Dong, et al., Total flavonoids from *Clinopodium chinense* (Benth.) O. Ktze protect against doxorubicin-induced cardiotoxicity *In vitro* and *In vivo*, Evid. Based Complement Altern. Med. 2015 (2015) 472565.
[9] S.E. Lipshultz, J.A. Alvarez, R.E. Scully, Anthracycline associated cardiotoxicity in survivors of childhood cancer, Heart 94 (2008) 525–533.
[10] L. Rochette, C. Guenancia, A. Gudjoncik, O. Hachet, M. Zeller, Y. Cottin, et al., Anthracyclines/trastuzumab: new aspects of cardiotoxicity and molecular mechanisms, Trends Pharmacol. Sci. 36 (2015) 326–348.
[11] R.M. Damiani, D.J. Moura, C.M. Viau, R.A. Caceres, J.A.P. Henriques, J. Saffi, Pathways of cardiac toxicity: comparison between chemotherapeutic drugs doxorubicin and mitoxantrone, Arch. Toxicol. 90 (2016) 2063–2076.
[12] H. Xiang, X. Tao, S. Xia, J. Qu, H. Song, J. Liu, et al., Targeting microRNA function in acute pancreatitis, Front. Physiol. 8 (2017) 726.
[13] S. De Rosa, A. Curcio, C. Indolfi, Emerging role of micrornas in cardiovascular diseases, Circ. J. 78 (2014) 567–575.
[14] S. De Rosa, C. Indolfi, Circulating microRNAs as biomarkers in cardiovascular diseases, EXS 106 (2015) 139–149.
[15] H. Xiang, X. Tao, S. Xia, J. Qu, H. Song, J. Liu, et al., Emodin alleviates sodium taurocholate-induced pancreatic acinar cell injury via MicroRNA-30a-5p- mediated inhibition of high-temperature requirement A/transforming growth factor beta 1 inflammatory signaling, Front Immunol. 8 (2017) 1488.
[16] X. Zhang, A. Chang, Y. Li, Y. Gao, H. Wang, Z. Ma, et al., miR-140-5p regulates adipocyte differentiation by targeting transforming growth factor-β signaling, Sci. Rep. 5 (2015) 18118.
[17] H. Lan, W. Chen, G. He, S. Yang, miR-140-5p inhibits ovarian cancer growth partially by repression of PDGFRA, Biomed. Pharmacother. 75 (2015) 117–122.

[18] R. Akhter, Y. Shao, M. Shaw, S. Formica, M. Khrestian, J.B. Leverenz, et al., Regulation of ADAM10 by miR-140-5p and potential relevance for Alzheimer's disease, Neurobiol. Aging 63 (2017) 110–119.

[19] L. Zhao, Y. Qi, L. Xu, X. Tao, X. Han, L. Yin, et al., MicroRNA-140-5p aggravates doxorubicin-induced cardiotoxicity by promoting myocardial oxidative stress via targeting Nrf2 and Sirt2, Redox Biol. 15 (2017) 284–296.

[20] M. Ge, W. Yao, Y. Wang, D. Yuan, X. Chi, G. Luo, et al., Propofol alleviates liver oxidative stress via activating Nrf2 pathway, J. Surg. Res. 196 (2015) 373–381.

[21] K.K. Nordgren, K.B. Wallace, Keap1 redox-dependent regulation of doxorubicin-induced oxidative stress response in cardiac myoblasts, Toxicol. Appl. Pharmacol. 274 (2014) 107–116.

[22] C. Luo, E. Urgard, T. Vooder, A. Metspalu, The role of COX-2 and Nrf2/ARE in anti-inflammation and antioxidative stress: aging and anti-aging, Med. Hypotheses 77 (2011) 174–178.

[23] S. Matsushima, J. Sadoshima, The role of sirtuins in cardiac disease, Am. J. Physiol. Heart Circ. Physiol. 309 (2015) H1375–H1389.

[24] L. Yin, Y. Xu, L. Xu, Y. Qi, X. Han, J. Peng, A green and efficient protocol for industrial -scale preparation of dioscin from *Dioscorea nipponica* Makino by two-step macroporous resin column chromatograph, Chem. Eng. J. 165 (2013) 281–289.

[25] J. Cho, H. Choi, J. Lee, M.S. Kim, H.Y. Sohn, D.G. Lee, The antifungal activity and membrane-disruptive action of dioscin extracted from *Dioscorea nipponica*, Biochim. Biophys. Acta 1828 (2013) 1153–1158.

[26] M.J. Hsieh, T.L. Tsai, Y.S. Hsieh, C.J. Wang, H.L. Chiou, Dioscin-induced autophagy mitigates cell apoptosis through modulation of PI3K/Akt and ERK and JNK signaling pathways in human lung cancer cell lines, Arch. Toxicol. 87 (2013) 1927–1937.

[27] H. Li, W. Huang, Y.Q. Wen, G.H. Gong, Q.B. Zhao, G. Yu, Anti-thrombotic activity and chemical characterization of steroidal saponins from *Dioscorea zingiberensis* C.H. Wright, Fitoterapia 81 (2010) 1147–1156.

[28] X. Zhang, L. Xu, L. Yin, Y. Qi, Y. Xu, X. Han, et al., Quantitative chemical proteomics for investigating the biomarkers of dioscin against liver fibrosis caused by CCl_4 in rats, Chem. Commun. 51 (2015) 11064–11067.

[29] L. Gu, X. Tao, Y. Xu, X. Han, Y. Qi, L. Xu, et al., Dioscin alleviates BDL- and DMN-induced hepatic fibrosis via Sirt1/Nrf2-mediated inhibition of p38 MAPK pathway, Toxicol. Appl. Pharmacol. 292 (2016) 19–29.

[30] M. Qi, L. Zheng, Y. Qi, X. Han, Y. Xu, L. Xu, et al., Dioscin attenuates renal ischemia/ reperfusion injury by inhibiting the TLR4/MyD88 signaling pathway via up- regulation of HSP70, Pharmacol. Res. 100 (2015) 341–352.

[31] X. Tao, X. Sun, L. Yin, X. Han, L. Xu, Y. Qi, et al., Dioscin ameliorates cerebral ischemia/ reperfusion injury through the downregulation of TLR4 signaling via HMGB-1 inhibition, Free Radic. Biol. Med. 84 (2015) 103–115.

[32] M. Liu, Y. Xu, X. Han, L. Yin, L. Xu, Y. Qi, et al., Dioscin alleviates alcoholic liver fibrosis by attenuating hepatic stellate cell activation via the TLR4/MyD88/NF-κB signaling pathway, Sci. Rep. 5 (2015) 18038.

[33] J. Qin, Y. Kang, Z. Xu, C. Zang, B. Fang, X. Liu, Dioscin prevents the mitochondrial apoptosis and attenuates oxidative stress in cardiac H9c2 cells, Drug Res. 64 (2014) 47–52.

[34] A.A. Elberry, A.B. Abdel-Naim, E.A. Abdel-Sattar, A.A. Nagy, H.A. Mosli, A.M. Mohamadin, et al., Cranberry (Vaccinium macrocarpon) protects against doxorubicin- induced cardiotoxicity in rats, Food Chem. Toxicol. 48 (2010) 1178–1184.

[35] Y.P. Yuan, Z.G. Ma, X. Zhang, S.C. Xu, X.F. Zeng, Z. Yang, et al., CTRP3 protected against doxorubicin-induced cardiac dysfunction, inflammation and cell death via activation of Sirt1, J. Mol. Cell Cardiol. 114 (2017) 38–47.

[36] W.N. Li, Z.Y. Qian, Effects of crocetin on cardiotoxicity of doxorubicin in rats, Chin. J. New Drugs 14 (2005) 1166–1169.

[37] D. Jain, Cardiotoxicity of doxorubicin and other anthracycline derivatives, J. Nucl. Cardiol. 7 (2000) 53–62.

[38] L.X. Fu, F. Waagstein, A. Hjalmarson, A new insight into adriamycin-induced cardiotoxicity, Int. J. Cardiol. 29 (1990) 15–20.

[39] P.K. Singal, N. Iliskovic, Adriamycin cardiomyopathy, N. Engl. J. Med. 339 (1998) 900–905.

[40] Y. Zhang, X. Tao, L. Yin, L. Xu, Y. Xu, Y. Qi, et al., Protective effects of dioscin against cisplatin-induced nephrotoxicity via the microRNA-34a/sirtuin 1 signalling pathway, Br. J. Pharmacol. 174 (2017) 2512–2527.

[41] L. Zheng, L. Yin, L. Xu, Y. Qi, H. Li, Y. Xu, et al., Protective effect of dioscin against thioacetamide-induced acute liver injury via FXR/AMPK signaling pathway in vivo, Biomed. Pharmacother. 97 (2018) 481–488.

[42] Y. Zhang, Y. Xu, Y. Qi, L. Xu, S. Song, L. Yin, et al., Protective effects of dioscin against doxorubicin-induced nephrotoxicity via adjusting FXR-mediated oxidative stress and inflammation, Toxicology 378 (2017) 53–64.

[43] Y. Qiao, L. Xu, X. Tao, L. Yin, Y. Qi, Y. Xu, et al., Protective effects of dioscin against fructose-induced renal damage via adjusting Sirt3-mediated oxidative stress, fibrosis, lipid metabolism and inflammation, Toxicol. Lett. 284 (2017) 37–45.

[44] M.C. Lin, M.C. Yin, Preventive effects of ellagic acid against doxorubicin-induced cardio-toxicity in mice, Cardiovasc Toxicol. 13 (2013) 185–193.

[45] Y. Maejima, J. Kuroda, S. Matsushima, T. Ago, J. Sadoshima, Regulation of myocardial growth and death by NADPH oxidase, J. Mol. Cell Cardiol. 50 (2011) 408–416.

[46] P.H. Sugden, A. Clerk, Oxidative stress and growth-regulating intracellular signaling pathways in cardiac myocytes, Antioxid. Redox Signal. 8 (2006) 2111–2124.

[47] Y. Yang, T. Yu, S. Jiang, Y. Zhang, M. Li, N. Tang, et al., Mirnas as potential therapeutic targets and diagnostic biomarkers for cardiovascular disease with a particular focus on wo2010091204, Expert Opin. Ther. Pat. 1–9 (2017).

[48] K.Y. Hasahya Tony, Q. Zeng, Microrna-208a silencing attenuates doxorubicin induced myocyte apoptosis and cardiac dysfunction, Oxid. Med. Cell Longev. 2015 (2015) 597032.

[49] J.X. Wang, X.J. Zhang, C. Feng, T. Sun, K. Wang, Y. Wang, et al., Microrna-532-3p regulates mitochondrial fission through targeting apoptosis repressor with caspase recruitment domain in doxorubicin cardiotoxicity, Cell Death Dis. 6 (2015) e1677.